small NANO MICRO

Graphene Devices

Structured Graphene Devices for Mass Transport

*Amelia Barreiro, Riccardo Rurali, Eduardo R. Hernández, and Adrian Bachtold**

The reversible atomic-mass transport along graphene devices has been achieved. The motion of Al and Au in the form of atoms or clusters is driven by applying an electric field between the metal electrodes that contact the graphene sheet. It is shown that Al moves in the direction of the applied electric field whereas Au tends to diffuse in all directions. The control of the motion of Al is further demonstrated by achieving a 90° turn, using a graphene device patterned in a crossroads configuration. The controlled motion of Al is attributed to the charge transfer from Al onto the graphene so that the Al is effectively charged and can be accelerated by the applied electric field. To get further insight into the actuation mechanism, theoretical simulations of individual Al and Au impurities on a perfect graphene sheet were performed. The direct (electrostatic) force was found to be ~1 pN and dominant over the wind force. These findings hold promise for practical use in future mass transport in complex circuits.

1. Introduction

One important goal of nanoscience is the development of robust experimental techniques for the controlled delivery of material at the nanoscale. A celebrated example is the manipulation of individual atoms with the tip of a scanning tunneling microscope, but this method is not readily automatized nor scalable to large numbers of atoms.[1] Recently, several groups have succeeded in conveying mass along carbon nanotubes, the atoms being transported by applying an electron current through the nanotube.[2–9] References [2–4] have demonstrated the transport of more than 10^7 atoms. These experiments were possible because nanotubes are mechanically robust and chemically inert so they can sustain the large current necessary for inducing mass transport. When using other materials, the tracks are easily damaged by the high current intensity.

Graphene is also expected to be an excellent mass conveyor; it is made of the same carbon sp^2 bonds as carbon nanotubes and it can transport similar current densities.[10–12] In contrast to nanotubes, however, graphene offers the advantage that its shape can be structured using conventional lithography techniques, so that one could envision the development of complex circuits for mass transport. However, the possibility of mass transport along graphene has not been demonstrated thus far, even in the simple configuration of straight ribbons.

We report on the motion of Al and Au along graphene tracks. The motion takes place in the form of individual atoms or clusters of atoms. We show that Al moves in the direction of the applied electric field, irrespective of the level of doping of the graphene, whereas Au tends to diffuse in all directions. In graphene devices patterned in a crossroads geometry, we were able to drive Al in a right angle turn by changing the direction of the electric field. The different behaviors observed for Al and Au are attributed to the charge transfer between these metals and the graphene. The charge transfer is expected to be more important in the case of Al, so it is effectively charged and can be actuated by the electric field applied between the two electrodes that electrically connect

Dr. A. Barreiro, Prof. A. Bachtold
CIN2 (ICN-CSIC) Barcelona, Campus UAB
E-08193 Bellaterra, Spain
E-mail: adrian.bachtold@cin2.es
Dr. A. Barreiro
Kavli Institute of Nanoscience
Delft University of Technology
PO Box 5046, 2600 GA, Delft, The Netherlands
Dr. R. Rurali
Institut de Ciència de Materials de Barcelona (ICMAB-CSIC)
Campus de Bellaterra
08193 Bellaterra, Spain
Dr. E. R. Hernández
Instituto de Ciencia de Materiales de Madrid (ICMM-CSIC)
Campus de Cantoblanco, E-28049 Madrid, Spain

DOI: 10.1002/smll.201001916

© 2011 Wiley-VCH Verlag GmbH & Co. KGaA, Weinheim

the graphene layer. Au remains mostly uncharged, on the other hand, and its motion is likely to be Brownian; the effect of the applied current being to Joule-heat graphene and enhance diffusion. To get further insight into the underlying mechanism of the actuation, we carried out numerical simulations on individual Al and Au impurities on a graphene sheet. These simulations show that Al atoms move due to the direct electrostatic force of electromigration, namely $q_{eff}\mathbf{E}$, where q_{eff} is the effective charge of the Al atoms and $\mathbf{E}$ is the electric field applied between the two electrodes. The associated force is estimated to be on the order of 1 pN. The wind force exerted by the charge carriers on the impurities is rather weak, and does not significantly affect the motion.

2. Experimental Results

We fabricated graphene devices with a conventional layout. A single graphene layer is electrically contacted to Cr/Au electrodes and the highly doped silicon wafer is used as the backgate. We also patterned Al or Au rectangular plates (about 500 nm wide and 50 nm thick) onto the graphene layer to supply atoms for mass transport.

To move the Al or Au atoms, we applied a large electric field along the graphene layer up to ~10 V μm^{-1}. The experiments were carried out in the vacuum of a scanning electron microscope (~10^{-6} mbar). The electric field was obtained by applying a voltage difference between the contact electrodes using micromanipulators. The large electric field generates an intense electrical current, which can be as high as ~10^8 A cm^{-2} (the current-carrying capacity of Al or Au wires is several orders of magnitude lower). Due to these extreme conditions the Al and Au plates fabricated on top of graphene tend to loose their original shape and some of the released metal propagates along the graphene nanoribbon.

The disintegration of the plates and the diffusive motion of the metal were imaged using scanning electron microscopy (SEM). **Figure 1** shows a selection of successive images of the motion of the aluminum. The Al is first released from the plate onto the graphene layer where it then propagates towards the electrode. Eventually, most of the Al disappears from the graphene layer. During the diffusion along the graphene, brighter spots can be observed (10–100 nm in size), which are assigned to larger pieces of Al. A careful inspection of our images (see Supporting Information) reveals the following tendency: Initially these pieces are small in size and tend to grow with time, but eventually the growth process is reversed and the pieces shrink, and in some cases are even seen to disappear. A similar behavior was observed in experiments on current-biased carbon nanotubes covered with indium particles (10–100 nm in size). The interpretation was that the indium atoms are driven in one direction along the nanotube from one particle to another one, so that the first particle gets smaller and the other one larger.[2] We explain our experiments in the same way, namely, the Al diffuses along the graphene, likely in the form of individual atoms or small clusters. However, a fraction of the metal atoms may also be lost due to evaporation as a result of the high temperatures reached by current-annealing.[10,13] Control experiments without Au/Al plates on the graphene were carried out, and we found no evidence of mass transport.

We observed that the motion of the Al (and the Au) was easy to drive at the beginning of the experiments, but became more difficult after some time (even when increasing the electric field to larger intensities), probably because of the contamination of the surface with amorphous carbon when imaging with the SEM. To minimize contamination, images were recorded as fast as possible and after setting the current to zero. Though unavoidable, the presence of a certain amount of amorphous carbon on the graphene ribbon does not seem to completely hinder the motion of Al and Au; however, repeated imaging

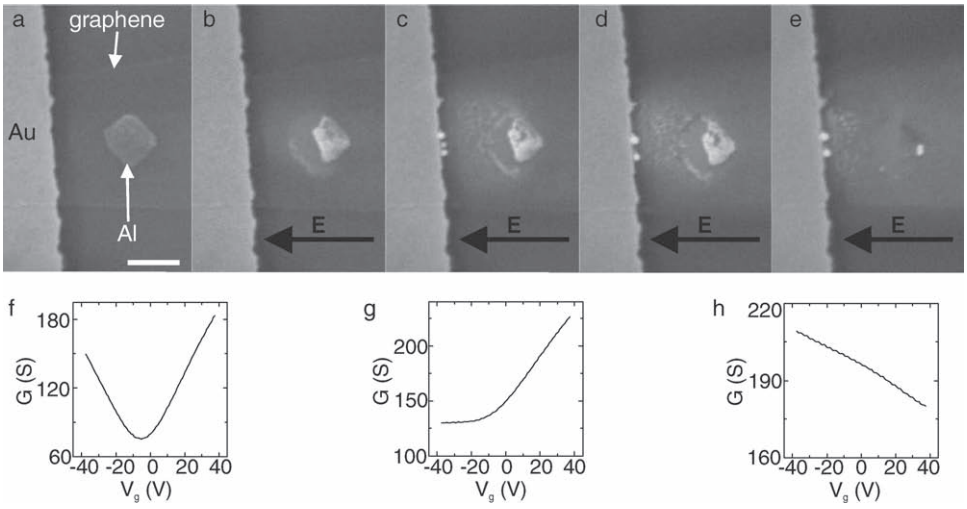

Figure 1. a) SEM image of a graphene device with one Al plate. The scale bar represents 400 nm. b–e) Motion of the aluminum after applying an electric field of different strengths. The arrow indicates the direction of the electric field. In (b) we applied a voltage V of 10.3 V for t = 5 min and the current I was 1.4 mA; in (c) V = 12.1 V, I = 1.64 mA, t = 7 min; in (d) V = 14.7 V, I = 1.98 mA, t = 3 min; in (e) V = 16.35 V, I = 2.3 mA, t = 3 min. f–h) Conductance measured at V = 10 mV as a function of gate voltage. The measurement in (f) was recorded before taking the image in (a), (g) before (b), and (h) before (e). The full series of images can be found in the Supporting Information.

© 2011 Wiley-VCH Verlag GmbH & Co. KGaA, Weinheim

small NANO MICRO

of the samples will inevitably increase the amount of contamination, eventually obstructing the motion of the metal.

The released Al moves in the direction of the electric field. Indeed, **Figure 2** shows three different Al plates on one graphene device, and the released metal is found on the left side of the plates when applying the electric field towards the left direction (black arrows in Figure 2b). When reversing the direction of the electric field, the motion of the Al is towards the other side (Figure 2c). The full series of images is in the Supporting Information.

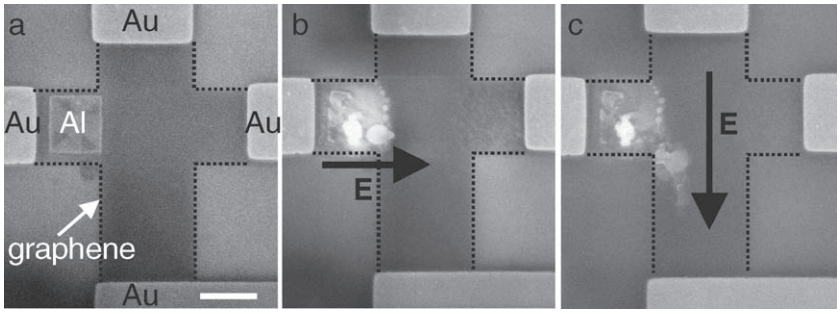

Figure 3. a) SEM image of a graphene device structured in a crossroads configuration with one Al plate. The scale bar represents 1 μm. b,c) Motion of the aluminum after applying an electric field in different directions (indicated by the arrow). In (b) we applied a voltage V of 9 V over $t = 6$ min and the current I was 1.4 mA; in (c) $V = 12.7$ V, $I = 1.63$ mA, $t = 9$ min.

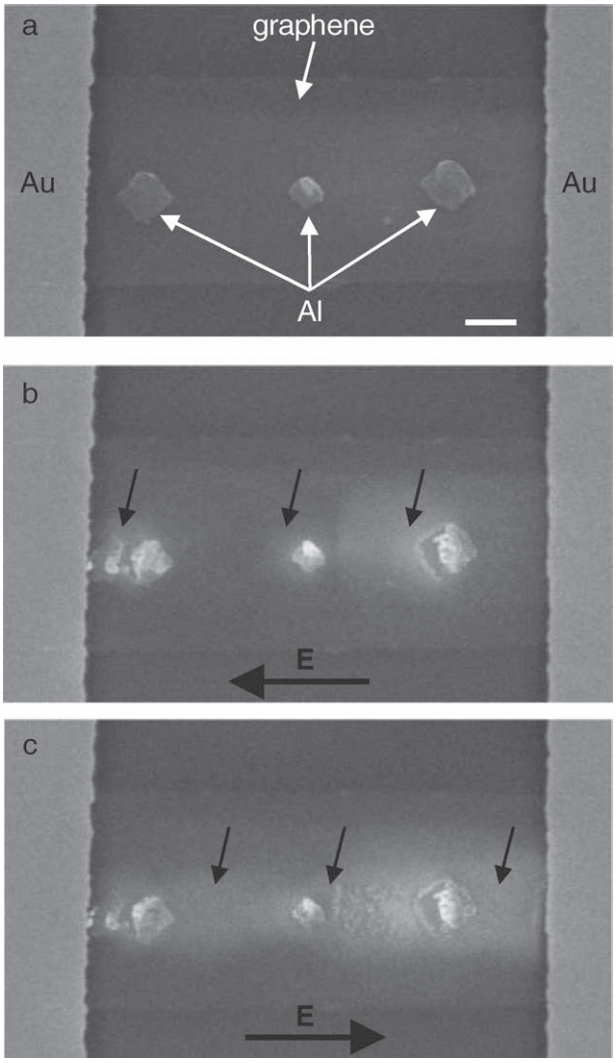

Figure 2. a) SEM image of a graphene ribbon contacted to two Au electrodes. Three square-shaped Al plates are lying on top of the graphene. The scale bar represents 500 nm. b) Motion of the aluminum after applying an electric field (whose direction is indicated by the long arrow). We applied a voltage of 15.3 V for 2 min (current = 2.2 mA). The displacement is highlighted with short arrows. c) Displacement of the aluminum in the opposite direction. We applied a voltage of 16.1 V for 5 min (current = 2.4 mA). The full series of images is in the Supporting Information.

We found that the motion of Al does not depend on whether the graphene charge carriers are electrons or holes. To evaluate the carrier type, we measured the conductance as a function of gate voltage, taking care that the applied voltage was below k_BT/e, where k_B is the Boltzmann constant, $T = 300$ K, and e the electronic charge. This electrical characterization was carried out each time before recording an image with the SEM. Figure 1 shows that the motion is always towards the direction of the electric field, while the graphene can be n doped or p doped (see Figure 1f–g). The progressive variation of the doping is a direct consequence of the large electrical current, as reported in Reference [10], but the microscopic mechanism of the variation of the doping is currently not understood.

Having characterized the actuation mechanism of Al atoms along graphene ribbons, we were in a position to develop a circuit for mass transport. The graphene was structured in a crossroads geometry and four electrodes were patterned in order to be able to apply the electric field in the horizontal or the vertical directions (**Figure 3**a). We drove the Al to make a right turn at the crossroads by first applying the electric field horizontally towards the right direction (Figure 3b) and then vertically towards the bottom direction (Figure 3c). The electric field was applied by voltage-biasing two opposite electrodes while leaving the remaining ones floating.

The motion of Au is markedly different from that of Al; the Au tends to diffuse in all directions (**Figure 4**), irrespective of the direction of the applied field. This isotropic diffusion was observed in all of the eight devices in which we studied the motion of Au (the devices had different lengths and widths). We also notice in Figure 4 a slight tendency of the Au to drift to the left, but this drift is weak and overall the motion is primarily affected by isotropic diffusion.

The disintegration of Au plates and that of Al plates are different as well. In the case of Au, the rectangular plate changes its form into a ball. This change is likely to be the result of the high temperature produced by Joule heating, which allows the plate to transform into a shape for which the surface-tension energy is reduced.[10,13] By contrast, the deteriorated Al plates tend to remain flat on the graphene, probably because the interaction of Al with graphene is stronger than that of Au.[14]

© 2011 Wiley-VCH Verlag GmbH & Co. KGaA, Weinheim

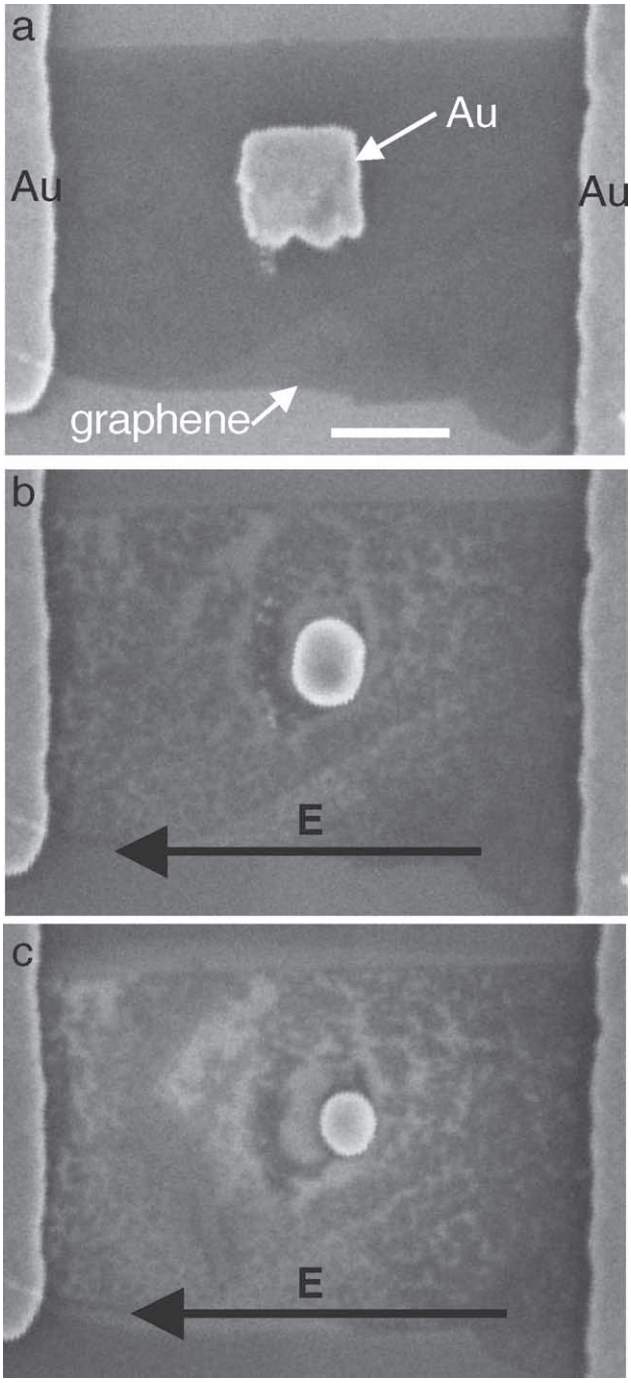

Figure 4. a) SEM images of a graphene device with one Au plate. The scale bar represents 400 nm. b,c) Motion of the gold after applying an electric field (direction indicated by the arrow). In (b) we applied a voltage V of 8.25 V over $t = 3$ min and the current I was 2 mA; in (c) $V = 9.87$ V, $I = 2.4$ mA, $t = 2$ min. The gold propagates in all directions.

3. Discussion

The observed mass transport may have an electrical or a thermal origin. Since the motion of Al can be reversed with the electric field, the underlying mechanism is electrical, a phenomenon known as electromigration.[15–18] The driving force in electromigration has been traditionally decomposed into the sum of a direct electrostatic force $\mathbf{F}_d$ and the so-called wind force $\mathbf{F}_w$.[15] The direct force is $\mathbf{F}_d = q_{eff}\mathbf{E}$. The wind force originates from the scattering of the charge carriers of graphene by the impurity atoms. This process results in a transfer of momentum from the scattered charge carriers to the impurities. The direction of the wind force depends on whether the carriers are electrons or holes.[19] In our experiments, the motion of Al does not depend on doping, which suggests that the direct force is dominant over the wind force. It is likely that the role of Joule heating is to make the directed diffusive motion faster.

As for Au, the atoms or small groups of atoms tend to diffuse in all directions, independent of the direction of the electric field. This observation suggests that electromigration is not the dominant mechanism in this case, but rather that the motion has a thermal origin. It is likely that the effect of the applied current is to increase the temperature of the graphene substrate via Joule heating and to increase the diffusion of Au atoms in all directions. Indeed, previous experiments have shown that the temperature significantly increases under similar experimental conditions. Reference [10] shows that the graphene sheet can reach about 600 °C by studying the melting of nearby semiconducting particles. A temperature of 400 °C was inferred from infrared and Raman spectroscopic measurements.[13]

Our finding that the origin of the motion of Al is electrical while that of Au is thermal can be attributed to the effective charge of Al and Au when placed on top of the graphene.[20] A first evaluation can be made using the work function of the different metals considered (4.1 eV for Al, 5.1 eV for Au, and ~5 eV for C). Electrons are expected to be transferred from Al to graphene (or amorphous carbon), leaving the Al positively charged. In contrast, the charge transfer between Au and C should be much weaker. This simple argument suggests that Al will be more susceptible to the electric field applied between the electrodes. The combined effect of a higher charge and a lower mass means that Al is electrically accelerated to a larger extent than Au, as indeed is observed in the experiments. Moreover, the fact that Al displays a clear tendency to move preferentially in the direction of the field is consistent with the prediction that the Al is positively charged.

4. Numerical Simulations

It is likely that multiple processes occur at the same time. For instance, the metal can move in the form of individual atoms or clusters, but can also be evaporated. In addition, the motion along the graphene can be hindered by amorphous carbon or other contamination. A complete picture of the microscopic nature of the motion is challenging to obtain for our experiment. Nevertheless, we theoretically analyze in the following the simplest possible case, namely, an individual Al or Au impurity on top of a perfect graphene sheet. This analysis allows us further insight into the actuation mechanism.

We have calculated the effective charge of Al and Au impurities placed on top of graphene sheets.[14,21] The calculations were performed using density-functional theory (see Supporting Information for computational details) and consisted of the following steps: We assumed clean graphene,

© 2011 Wiley-VCH Verlag GmbH & Co. KGaA, Weinheim

small NANO MICRO

which should be reasonable at least at the initial stages of the experiments, as directly involving contaminants in our calculations is currently not feasible. We optimized the position of Al and Au impurities on top of the graphene sheet, finding that Al is preferably adsorbed 2.1 Å above the center of a C hexagon, whereas Au is adsorbed 2.5 Å on top of a C atom. Next, we calculated the charge transfer between graphene and the atomic impurity by estimating the partial charge of each subsystem using Bader's Atoms in Molecules analysis.[22] In the case of Al impurities, we found that there is a charge transfer of 1.3 e, where e is the charge of the electron, from the impurity to the graphene layer (see **Figure 5**), while in the case of Au impurities, the charge transfer is lower, 0.1 e, and takes place in the opposite direction, i.e., from the graphene layer to the impurity (Figure 5b). The results of this charge-transfer analysis allow us to evaluate the force acting on the Al impurities. Using $q_{eff} = 1.3$ e and $\mathbf{E} = 10$ V μm^{-1}, we obtain a direct (electrostatic) force of about ~2 pN.

In the particular case of Al we have also performed calculations in voltage-biased graphene to mimic more closely the experimental situation. From these calculations we can extract an estimation of the total force $\mathbf{F}_{tot}$ acting on the impurity (see Supporting Information). This force includes a direct-force and a wind-force contribution, within the limits of approximation inherent to the calculation methodology.[15] We can employ our previous determination of the charge on the Al impurity to extract an estimation of the direct force; this we do as follows: One of the outcomes of the calculation is an electrostatic-potential drop in the direction of the current. By taking the resulting electric field multiplied by the charge of the impurity, admittedly a crude approximation, we can get an estimation of the magnitude of the direct force.[23] We can then extract a value for the wind force using $\mathbf{F}_w = \mathbf{F}_{tot} - \mathbf{F}e$. Our results are plotted in Figure 5c. As can be seen, the total force resulting on the Al impurity is nearly linear in bias. Whereas the direct-force contribution is negative, the wind-force contribution is positive. Namely, the wind force is directed in the opposite direction from the electric field. This is because the carriers in this case are electrons (the graphene was initially uncharged in the calculations, but Al induces n doping with ~10^{13} cm^{-2} charge concentration). More importantly, we obtain that the direct force is larger in strength than the wind force, albeit they are of the same order of magnitude. At $\mathbf{E} = 10$ V μm^{-1}, the wind force is ~0.4 pN. Given the nature of the approximations necessary to obtain these estimates, values should not be taken as quantitative but they are nevertheless consistent with our experimental finding that the direct force should be the dominant contribution.

To strengthen the result of these calculations, we use another estimate of the wind force. The wind force can be evaluated from the rate of momentum transfer by the charge carriers to the Al impurities.[24,25] Assuming that Al atoms act as Coulomb-scattering centers, which is justified by the large charge transfer calculated above, and taking the conical band structure of graphene, we obtain

$$\mathbf{F}_w = \pm \frac{n\mu}{n_{Al}\mu_{Al}} e\mathbf{E} \quad (1)$$

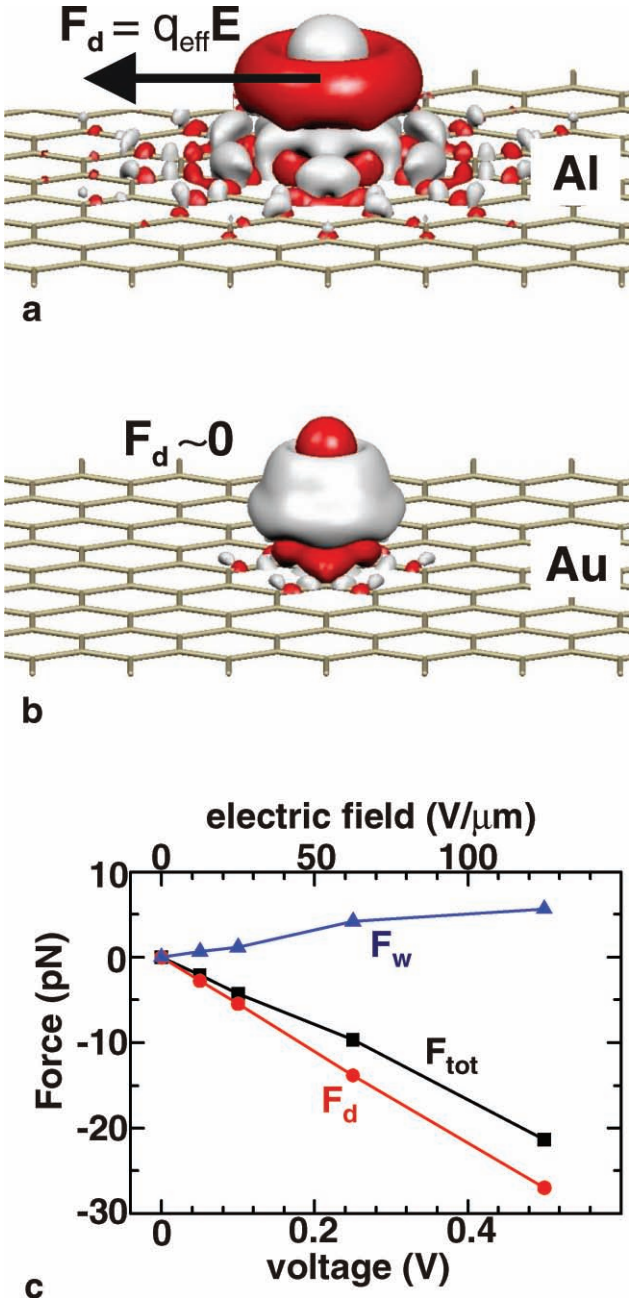

Figure 5. a,b) Charge-density-difference map for Al and Au impurities on graphene. Red indicates charge-density loss; white indicates increase. In the case of Al there is a significant charge transfer towards the graphene substrate (~1.3 e, see text); in this case the charged impurity is expected to sustain a large direct force contribution. In the case of Au impurities the charge transfer is significantly smaller (~0.1 e, see text), and therefore the direct-force contribution will be small. c) Total force on an Al impurity on graphene as a function of voltage bias. Also shown are estimates of the direct-force and wind-force contributions. The length of the graphene channel is 4 nm.

where n_{Al} is the concentration of Al atoms, n the carrier density, μ_{Al} the mobility associated to Al atoms, and μ the mobility related to the other impurities (see Supporting Information). The sign of the wind force depends on whether the carriers are holes or electrons. It has been shown that in the case of Coulomb scatterers the product of the mobility and the impurity

© 2011 Wiley-VCH Verlag GmbH & Co. KGaA, Weinheim

density is a constant, which to a first approximation depends only on the dielectric constant of the environment. In our configuration, we have $n_{Al} \cdot \mu_{Al} \approx 5 \cdot 10^{15}$ V^{-1} s^{-1}.[26,27] Taking the typical mobility of our fabricated devices (μ = 1000 cm^2 V^{-1} s^{-1}), $n \approx 0.5 - 5 \cdot 10^{12}$ cm^{-2}, and $\mathbf{E} = 10$ V µm^{-1}, the wind force is 0.1–1 pN, which is consistent with our previous estimation above.

5. Conclusion

In conclusion, we report on the motion of Al and Au along graphene devices. In the case of Al it is clearly shown that the actuation mechanism is the direct electrostatic force of electromigration, whereas the motion of Au atoms is dominated by thermal effects. The characterization of the actuation mechanism allowed us to fabricate a crossroads track where Al makes a right turn. This proof-of-principle experiment shows the potential of graphene to develop complex nanocircuits for mass transport. A more advanced detection scheme will be needed to probe the motion at the atomic scale, using, e.g., scanning-probe microscopy or high-resolution transmission electron microscopy.[28,29] Indeed, the scanning electron microscope that we used here cannot monitor the motion of single atoms. Tracking the motion of single atoms along graphene sheets would be necessary in future experiments to attain a detailed characterization of mass-transport phenomena. Such experiments could provide new data that may help to contrast the different theories of electromigration, which were developed by such eminent physicists as Friedel, Peierls, and Landauer, but thus far have not been tested experimentally in a quantitative way.[15,30–32] Indeed, previous experiments on bulk materials suffered from the difficulty of evaluating the electronic current at the surface that is experienced by impurities, whereas this problem is avoided in graphene since the current only flows at the surface.

6. Experimental Section

Graphene devices were assembled using standard nanofabrication techniques. Graphene flakes were obtained by mechanical exfoliation of Kish graphite (Toshiba Ceramics) on highly doped silicon wafers coated with a 280-nm thick thermal silicon oxide layer. Single layers were identified with optical microscopy and Raman spectroscopy. Graphene layers were structured using O_2 plasma etching into straight ribbons or crossroads. Cr/Au (7 nm/70 nm) electrodes were fabricated on top of the samples using electron-beam lithography, followed by a lift-off in acetone and dichloroethane. In a second lithography step we patterned Al or Au rectangular plates (about 500 nm wide and 50 nm thick) onto the graphene layer to supply the atoms for mass transport.

Supporting Information

Supporting Information is available from the Wiley Online Library or from the author.

Acknowledgements

We thank V. E. Calado, A. M. Goossens, X. Liu, J. Moser, M. Sledzinska, and L. M. K. Vandersypen for discussions, experimental help, and support. We acknowledge financial support by the European Commission (EURYI), the Spanish ministry (FIS2009–11284, TEC2009–06986, FIS2009–12721-C04–03, and CSD2007-00041), and the Catalan Generalitat (SGR2009).

[1] M. F. Crommie, C. P. Lutz, D. M. Eigler, *Nature* **1993**, *363*, 524.
[2] B. C. Regan, S. Aloni, R. O. Ritchie, U. Dahmen, A. Zettl, *Nature* **2004**, *428*, 924.
[3] K. Svensson, H. Olin, E. Olsson, *Phys. Rev. Lett.* **2004**, *93*, 145901.
[4] D. Goldberg, P. M. F. J. Costa, M. Mitome, S. Hampel, D. Haase, C. Mueller, A. Leonhardt, Y. Bando, *Adv. Mater.* **2007**, *19*, 1937.
[5] A. Barreiro, R. Rurali, E. R. Hernandez, J. Moser, T. Pichler, L. Forro, A. Bachtold, *Science* **2008**, *320*, 775.
[6] J. H. Warner, Y. Ito, M. Zaka, L. Ge, T. Akachi, H. Okimoto, K. Porfyrakis, A. A. R. Watt, H. Shinohara, G. A. D. Briggs, *Nano Lett.* **2008**, *8*, 2328.
[7] C. Jin, K. Suenaga, S. Iijima, *Nat. Nanotechnol.* **2008**, *3*, 17.
[8] G. E. Begtrup, W. Gannett, T. D. Yuzvinsky, V. H. Crespi, A. Zettl, *Nano Lett.* **2009**, *9*, 1835.
[9] A. Nagataki, T. Kawai, Y. Miyamoto, O. Suekane, Y. Nakayama, *Phys. Rev. Lett.* **2009**, *102*, 176808.
[10] J. Moser, A. Barreiro, A. Bachtold, *Appl. Phys. Lett.* **2007**, *91*, 163513.
[11] A. Barreiro, M. Lazzeri, J. Moser, F. Mauri, A. Bachtold, *Phys. Rev. Lett.* **2009**, *103*, 076601.
[12] D. H. Chae, B. Krauss, K. von Klitzing, J. H. Smet, *Nano Lett.* **2010**, *10*, 466.
[13] M. Freitag, H.-Y. Chiu, M. Steiner, V. Perebeinos, P. Avouris, *Nat. Nanotechnol.* **2010**, *5*, 497.
[14] K. T. Chan, J. B. Neaton, M. L. Cohen, *Phys Rev. B* **2008**, *77*, 235430.
[15] R. S. Sorbello, *Solid State Phys.* **1997**, *51*, 159.
[16] H. Yasunaga, A. Natori, *Surf. Sci. Rep.* **1992**, *15*, 205.
[17] N. Mingo, L. Yang, J. Han, *J. Phys. Chem. B* **2001**, *105*, 11142.
[18] Y. Girard, T. Yamamoto, K. Watanabe, *J. Phys. Chem. C* **2007**, *111*, 12478.
[19] S. Heinze, N. P. Wang, J. Tersoff, *Phys. Rev. Lett.* **2005**, *95*, 186802.
[20] Y. Ren, S. Chen, W. Cai, Y. Zhu, C. Zhu, R. S. Ruoff, *Appl. Phys. Lett.* **2010**, *97*, 053107.
[21] F. J. Ribeiro, J. B. Neaton, S. G. Louie, M. L. Cohen, *Phys. Rev. B* **2005**, *72*, 075302.
[22] R. F. W. Bader, in *Atoms in Molecules: A Quantum Theory,* Oxford University Press, Oxford, UK **1995**.
[23] The electrostatic potential includes oscillations due to the atomic cores of the carbon atoms and the impurity, but we are interested only in the effect of the bias-induced field, which we approximate by a linear interpolation to the electrostatic potential drop. The resulting electric field is close to the value obtained by dividing the applied voltage by the separation between the electrodes.
[24] R. S. Sorbello, *Phys. Rev. B* **1989**, *39*, 4984.
[25] H. B. Huntington, A. R. Grone, *J. Phys. Chem. Solids* **1961**, *20*, 76.
[26] S. Adam, E. H. Hwang, V. M. Galitski, S. Das Sarma, *Proc. Natl. Acad. Sci. USA* **2007**, *104*, 18392.
[27] J. H. Chen, C. Jang, S. Adam, M. S. Fuhrer, E. D. Williams, M. Ishigami, *Nat. Phys.* **2008**, *4*, 377.
[28] G. M. Rutter, J. N. Crain, N. P. Guisinger, T. Li, P. N. First, J. A. Stroscio, *Science* **2007**, *317*, 219.
[29] J. C. Meyer, Ç. Ö. Girit, M. F. Crommie, A. Zettl, *Nature* **2008**, *454*, 319.
[30] C. Bosvieux, J. Friedel, *J. Phys. Chem. Solids* **1962**, *23*, 123.
[31] A. K. Das, R. Peierls, *J. Phys. C* **1973**, *6*, 2811.
[32] R. Landauer, J. W. F. Woo, *Phys Rev. B* **1974**, *10*, 1266.

Received: October 27, 2010
Published online: February 1, 2011

© 2011 Wiley-VCH Verlag GmbH & Co. KGaA, Weinheim